REACTION-BONDED ZrO_2-TOUGHENED Al_2O_3 (ZT-RBAO)

Nils CLAUSSEN, Dietmar HOLZ, Suxing WU and Manfred RÜHLE*

Advanced Ceramics Group, Technische Universität Hamburg-Harburg, D-2100 Hamburg 90, Germany

ABSTRACT

The reaction bonding of Al_2O_3 is strongly affected by additions of either ZrO_2 or Zr metal. On the one hand, Y_2O_3-stabilized ZrO_2 considerably reduces the oxidation time making one-step reaction bonding possible, on the other hand, ZrO_2 leads to transformation toughening. Mechanically alloyed Al-Zr (+ Y_2O_3) compacts exhibit even faster reaction bonding behavior. The paper discusses the reaction mechanism and gives first results on ZrO_2-containing RBAO.

I. INTRODUCTION

Reaction forming of ceramics as an alternative to conventional processing has been of general interest for long. Various advantages, such as low processing temperatures, low raw material costs, near-net-shape tailorability, and glass-phase-free grain boundaries are most attractive for many technical and high-performance applications/1/. A few years ago, directed oxidation of molten metals (DMO) has been introduced/2,3/. In this technique, an Al_2O_3/Al composite is produced by oxidizing molten Al alloys. The most recently developed oxidation-forming technique is based on the reaction-bonding of Al_2O_3 (RBAO), essentially starting from a mixture of Al and Al_2O_3 powder/4-6/. This technology shows wide microstructural variability and a great application potential.

The purpose of this paper is to discuss the reaction bonding mechanism and to show the influence of ZrO_2/Zr additions on the reaction process, the microstructure and mechanical properties. Only preliminary results are available at present.

---

* Max-Planck-Institut für Metallforschung, Stuttgart, Germany

II. PRINCIPLES OF RBAO TECHNOLOGY

Al metal powder and Al_2O_3 powder, usually with 30 to 60 vol% Al, is intensively mixed in a ball mill with 3Y-TZP milling media such that the Al is reduced to small (~1 μm) particles with submicron Al_2O_3 and ZrO_2 dispersions. The ZrO_2 dispersions usually result from the wear of the milling balls (e.g., 3Y-TZP) while the Al_2O_3 originates both from the fines fraction of the admixed Al_2O_3 and the Al oxidation products caused by the milling process. Extensive milling in water would fully convert the Al into $Al(OH)_3$, hence milling is carried out in an organic milling fluid (e.g., acetone). In an open system, up to ~40 % of Al may still be oxidized for an optimized milling duration. This may be avoided in a closed milling system, as for instance used in the mechanical alloying of intermetallics/7/. After milling, the powder mixture is passivated such as to allow safe handling.

Any green compacting technique can be applied to form the required shapes. As shown schematically in Fig. 1, Al particles are plastically deformed which results in strong Al/Al contacts bridging the Al_2O_3 particles (Fig. 2). Green density is, therefore, high and green strength may attain values more than an order of magnitude higher (20 - 50 MPa) than those of conventional ceramic green bodies. On heating the compact in an oxidizing atmosphere (usually air) to temperatures between 800 to 1200°C, Al reacts to Al_2O_3 which is associated with a 28 % volume expansion (reaction stage). In the sintering stage at temperatures > 1200°C, the body shrinks compensating for the expansion in the reaction stage. The total dimensional changes during the complete process are small though. Oxidation actually starts below the melting point of Al, i.e., from temperatures ≥ 300°C, and most of the Al reacts in the first part of the reaction stage. Furthermore, sintering begins at relatively low temperatures (> 1200°C).

Completely reaction-bonded bodies usually exhibit 3 to 8 % homogeneously distributed micropores between grains of sizes <1 μm. The strength of RBAO samples is therefore higher than that of conventionally sintered Al_2O_3 bodies at a given density, e.g., >500 MPa at 94.5 % TD and 20 vol% 2Y-TZP content. The microstructure of the same composition isopressed at 100 MPa, oxidized and sintered in one step at 1600°C for 5 h is presented in Fig. 3. Even at such extended sintering periods, the grain size is ~1 μm which is mainly due to the grain growth inhibiting effect of the ZrO_2 particles (dark in Fig. 3). Added and newly formed Al_2O_3, however, can no longer be differentiated unter these processing conditions/8/.

The RBAO process can be modified in various ways by either metal (e.g., Zr, Cr, Si) or ceramic additives (e.g., ZrO_2, Cr_2O_3, MgO, SiC, etc.). The main purpose of ZrO_2 or Zr is to enhance the oxidation process and that of the other constituents is to further compensate for the sintering shrinkage by extended expansions during the reaction stage. (see Table 1).

III. REACTION BONDING MECHANISMS

The exact mechanisms taking place in the RBAO process have yet to be analyzed, however, various details can be described, and it appears obvious that they differ significantly from those occurring in the DMO process. From thermogravimetrical and dilatometer analyses it can be shown that between room temperature and ~300°C, weight loss reveals the evaporation of fugitive species; at T > ~300°C, oxidation of Al takes place demonstrated by a strong weight gain and an increased slope in the dilatometer curve. It is interesting to note that over 30 % of the Al-to-Al_2O_3 reaction proceeds as solid state/gas reaction. At ~600°, melting of Al occurs leading to a small drop in the expansion curve. Extensive particle rearrangement, e.g., as observed in liquid-phase sintering of WC-Co, is not observed after sufficient milling of the components. The oxide skin on the Al particles developed during milling and oxidation at T < 600°C, rather prevents much redistribution of molten Al. Above the melting point, further expansion due to reaction probably goes along with some particle rearrangement and the filling of voids by the oxide product. The reaction is usually completed during the first hold (1000 to 1150°C), i.e., the molten regions within the Al particles have fully been replaced by small (50 to 100 nm) Al_2O_3 crystals. Due to the extremely fine crystal size, sintering starts already at temperatures ≥1200°C.

Except for ZrO_2 or Zr, dopants, such as Mg, Si, Zn, are not required to initiate and sustain the reaction as is the case for the DMO process. Annealing at temperatures below the melting point may lead to nearly complete oxidation, however, it requires impractically long processing times. The facts that sustained oxidation at T < 600°C takes place and that the incubation period and the channel system associated with the growth of DMO products are lacking, are evidence for different oxidation mechanisms prevailing DMO and RBAO processes.

The schematic diagram in Fig. 4 demonstrates the suggested mechanisms. In the first reaction period, oxygen can freely move through the open pore system of the compact. In case of air as oxydant, nitrogen would enrich adjacent to the newly formed Al_2O_3 coat

surrounding the Al particle. Oxygen diffuses along the grain boundaries which, due to the ultrafine grain size, offer an effective oxygen transport path. Oxidation of the molten inner part of the Al particles can thus proceed. Because of the 28 % volume expansion resulting from Al oxidation, the pressure in the molten Al pool increases until the scale fractures and Al spills into the void space of the neighbouring particles. Due to the bad wetting of Al_2O_3 (or ZrO_2) by liquid Al, a droplet forms which is readily coated by an oxide skin again. This process continues until all Al has been oxidized. This could be demonstrated by TEM analyses/5,8/.

As also indicated in Fig. 4, ZrO_2 particles assist in transporting oxygen to the Al particles by lattice diffusion. During oxidation in air, this selective O^{2-} diffusion reduces the probability of N_2 clogging the oxygen access. Especially in the later oxidation stage, i.e., when pores close due to early sintering of the nanometer-sized Al_2O_3 crystals, thorough and rapid oxidation of the RBAO body is guaranteed.

In the sintering stage, "old" Al_2O_3 particles are bonded and grain growth, mainly of the "new" crystals, takes place. The final dimensional change between green and fully reaction bonded state essentially depends on Al/Al_2O_3 ratio, green density, and heat-treatment cycle.

IV. ZrO_2-CONTAINING RBAO

Various preliminary experiments have been carried out in order to study the effect of Y_2O_3-stabilized and unstabilized ZrO_2 as well as metallic Zr on the RBAO process and the mechanical properties. The starting materials and the compositions investigated are listed in Tables 2 and 3. In the following, a summary is presented on these results. Details will be given elsewhere/8,9/.

The pore size distribution of RBAO green bodies containing 30 vol% ZrO_2 (composition I, cf. Table 3) is given in Fig. 5 as a function of isostatic compaction pressure. The mean pore size decreases from 50 nm at 100 MPa to 10 nm at 900 MPa. This high compaction pressure results in a green strength of > 60 MPa as revealed in Fig. 6. It is interesting to note that the green strength of unmilled powder compacts is much lower than that of mechanically alloyed powder compacts. After reaction at 1100°C for 10 h and sintering at 1400°C for 5 h, strength and toughness of RBAO samples containing 15 vol% unstabilized ZrO_2 (composition II, cf. Table 3) decrease with compaction pressure (Fig. 7). The reaction behavior of these samples is not improved as

compared to ZrO_2-free RBAO which may be explained by the lower vacancy concentration of unstabilized ZrO_2 as compared to Y_2O_3-stabilized ZrO_2. The relatively low strength is mainly due to spontaneous transformation to monoclinic symmetry.

When Y_2O_3-stabilized ZrO_2 is used, as e.g. introduced by the milling ball wear, the reaction process is very much accellerated. This effect of ZrO_2 is also true for SiC-containing compositions that react to mullite/10/. The possible mechanism for this fact has been discussed in chapter IV. Samples containing 20 vol% $2Y_2O_3$-stabilized ZrO_2 (composition III, cf. Table 3) reacted for 2 h at 1200°C and sintered for 5 h at 1550°C, exhibit strengths of > 500 MPa at only 94.5 % TD. This strength is superior to that of conventionally sintered ZTA at the same density, mainly due to the homogeneous distribution of micropores. It must be pointed out that similar compositions can be reaction sintered in one step, e.g., by heating with a rate of 10 K/min to 1500°C and holding for 2 h, densities of > 95 % TD were obtained. Such samples HIPed at 1500°C and 200 MPa in Ar for 15 min lead to > 99 % TD and strengths of > 1100 MPa.

The most effective additive for the RBAO process seems to be Zr metal which, when mechanically alloyed with Al, enables even fast firing without fracturing the samples. Obviously, the oxidation is even more disruptive than when ZrO_2 is present. E.g., compositions consisting of 35 vol% Al, 20 vol% Zr mixed with Y_2O_3 to result in 3Y-TZP on oxidation and 45 vol% Al_2O_3 (composition IV, cf. Table 3), isopressed at 600 MPa were heated in one step to 1580°C for 30 min. A density of > 97 % TD was achieved with most of the ZrO_2 being in tetragonal symmetry. Since the oxidation of Zr to ZrO_2 is associated with a 49 % volume expansion, compensation to the sintering shrinkage allows for even better near-net shape fabricability than when ZrO_2 is added to the RBAO precursor.

V. CONCLUSIONS

The following conclusions are based not only on the text of this extended abstract, but also on other experimental results mentioned in the literature quoted:

a) Oxidation of RBAO green bodies proceeds "self-disruptive" and not "dopant-disruptive" as in DMO processing.
b) Oxidation takes place by oxygen grain boundary diffusion through the newly formed, fine (~10 to 100 nm) Al_2O_3 crystals. The oxygen is transported either

through the gas phase or through the lattice of ZrO_2 particles.

c) Wettability of Al_2O_3 (or ZrO_2) by Al is not required and an incubation period as in DMO does not exist.

d) Y_2O_3-stabilized tetragonal ZrO_2 additions strongly reduce the reaction-bonding time.

e) Mechanically alloyed Zr/Al (Zr-added instead of ZrO_2) is even more effective than ZrO_2 in enhancing the reaction process.

f) Both ZrO_2 and Zr (+ Y_2O_3) additions lead to transformation toughening.

g) Unstabilized ZrO_2 additions have shown to be little effective in improving the RBAO process. This is partially due to spontaneous transformation to monoclinic symmetry.

ACKNOWLEDGEMENT

The authors thank Deutsche Forschungsgemeinschaft (DFG) for financial support under contract No. Cl 52/13-1.

REFERENCES

/1/ J.S. Haggerty and Y.-M. Chiang, "Reaction-Based Processing Methods of Ceramics and Composites", Ceram.Eng.Sci.Proc. 11 (1-8), 757-94 (1990).

/2/ M.S. Newkirk, A.W. Urquhart, H.R. Zwicker, and E. Breval, "Formation of Lanxide Ceramic Composite Materials", J.Mater.Res. 1, 81-89 (1986).

/3/ N. Claussen and A.W. Urquhart, "Directed Oxidation of Molten Metals", in "Encyclopedia of Mat. and Eng." (Ed. R.W. Cahn), Supplementary Vol. 2, Pergamon, Oxford, 1111-5 (1990).

/4/ N. Claussen, Tuyen Le, and Suxing Wu, "Low Shrinkage Reaction-Bonded Alumina", J.Eur.Ceram. Soc., 5, 29-35 (1989).

/5/ N. Claussen, N.A. Travitzky, and Suxing Wu, "Tailoring of Reaction-Bonded Al_2O_3 (RBAO) Ceramics", Ceram.Eng.Sci.Pro., 11, 806-820 (1990).

/6/ Suxing Wu, N.A. Travitzky, and N. Claussen, "Processing of Reaction-Bonded Al_2O_3 (RBAO) Composites", in "Structural Ceramics - Processing, Microstructure, and Properties", (Eds.J.J. Bentzen et al.), Roskilde, Denmark, 529-534 (1990).

/7/ M. Oehring and R. Bormann, "Nanocrystalline Alloys Prepared by Mechanical Alloying and Ball Milling", to be published in Mat.Sci.and Eng. A 132 (1991).

/8/ M. Rühle, Suxing Wu, and N. Claussen, "Microstructure Analysis of RBAO Ceramics", to be published.

/9/ D. Holz, PhD work being performed at TUHH, Advanced Ceramics Group.

/10/Suxing Wu and N. Claussen, "Fabrication and Properties of Low-Shrinkage Reaction-Bonded Mullite", submitted to J.Am.Ceram.Soc.

Reaction			Δ V , %
Mg	→	MgO	- 19
$Al_2O_3 + SiO_2$	→	$3Al_2O_3 \cdot 2SiO_2$ (mullite)	+ 13
Al	→	Al_2O_3	+ 28
Zr	$\xrightarrow{Y_2O_3}$	t-ZrO_2	+ 49
Zn	→	ZnO	+ 58
Ni	→	NiO	+ 70
Co	→	CoO	+ 75
Ti	→	TiO_2	+ 76
Cu	→	CuO	+ 86
Si_3N_4	→	SiO_2	+ 90
Cr	→	Cr_2O_3	+ 102
SiC	→	SiO_2	+ 108
Si	→	SiO_2	+ 115

Table 1 : Volume expansion of some metals on oxidation

Al

Alcan 105	Alcan-Toyo America, Incorporation, USA 2.702 g/cm^3, 5-50 µm, 99.77 %

Al_2O_3

Al-PC13	Showa Aluminum Industries, Tokyo, Japan 3.97 g/cm^3, 13 µm, Platelets
Atochem 15-25	Atochem, Pierre-Benite, France 3.97 g/cm^3, 15-25 µm, Platelets
Dycron 13	Hüls AG, Marl, FRG 3.97 g/cm^3, 13 µm, Platelets
Ceralox HPA-0.5	Condea Chemie GmbH, Brunsbüttel, FRG 3.97 g/cm^3, 0.5 µm, > 99.9 %
Ceralox MPA-4	Condea Chemie GmbH, Brunsbüttel, FRG 3.97 g/cm^3, 4 µm, > 99.9 %

ZrO_2

Dynazirkon F	Dynamit Nobel, Sweden 5.7 g/cm^3, 0.7 µm, ZrO_2+HfO_2 99.7 %, unstabilized
TZ-2Y	Tosoh Corporation, Tokyo, Japan 6.11 g/cm^3, 17.8 m^2/g, 96.4 %, 2 mole% Y_2O_3

Additives

Mg	E. Merck, Darmstadt, FRG 1.74 g/cm^3, < 100 µm, 97 %
Zn	E. Merck, Darmstadt, FRG 7.14 g/cm^3, < 60 µm, 95 %
Zr	E. Merck, Darmstadt, FRG 6.3 g/cm^3, < 40 µm, 80 %
SiO_2	Sigma Chemical Company, St. Louis, USA 2.5 g/cm^3, 0.5-10 µm, 99 %
Y_2O_3	H. C. Starck, Berlin, FRG 5.01 g/cm^3, 0.5 µm, 99.8 %

Table 2: Starting materials of ZrO_2-toughened RBAO

No.	Composition	Material
I	60 vol% Al	Alcan 105
	10 vol% Al_2O_3	Al-PC13
	30 vol% ZrO_2	TZ-2Y
II	40 vol% Al	Alcan 105
	+ 12 wt% SiO_2	Sigma
	+ 2.5 wt% Mg	E. Merck
	+ 0.1 wt% Zn	E. Merck
	45 vol% Al_2O_3	Dycron 13
	15 vol% ZrO_2	Dynazirkon F
III	35 vol% Al	Alcan 105
	40 vol% Al_2O_3	Ceralox HPA-0.5
	5 vol% Al_2O_3	Atochem 15-25
	20 vol% ZrO_2	TZ-2Y
IV	35 vol% Al	Alcan 105
	40 vol% Al_2O_3	Ceralox MPA-4
	5 vol% Al_2O_3	Atochem 15-25
	20 vol% Zr	E. Merck
	+ 7 wt% Y_2O_3	H.C. Starck

Table 3: Compositions of ZrO_2-toughened RBAO

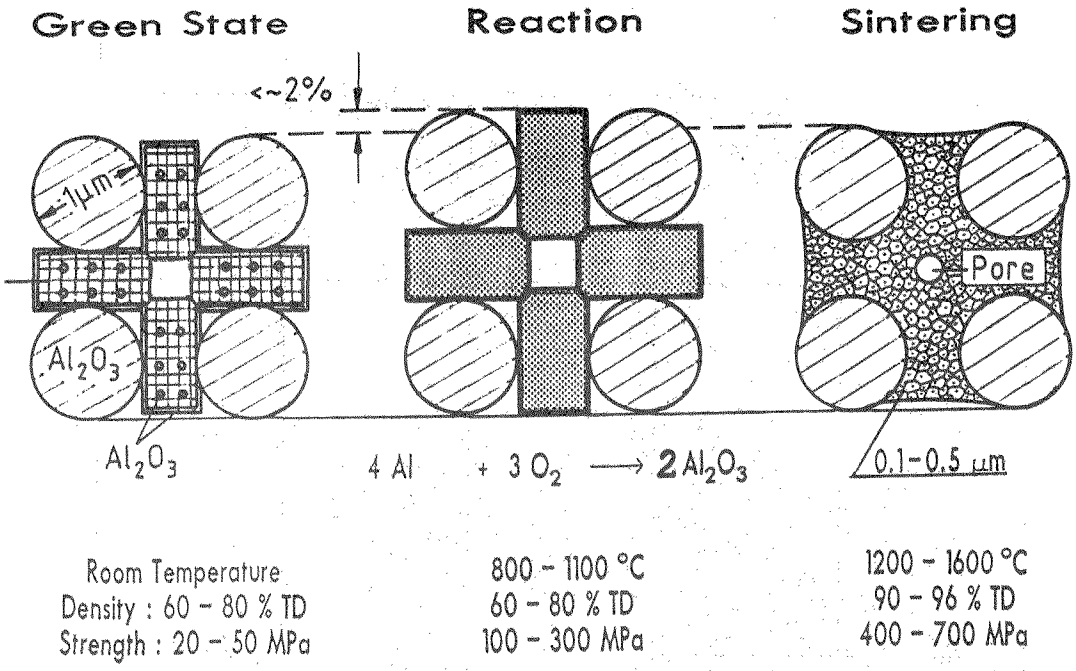

Fig. 1. Schematic diagram of the RBAO process. In the green state, "old" Al_2O_3 particles are bridged by contacting Al particles containing oxide dispersions from mechanical alloying. In the reaction stage, associated with an expansion, the molten Al transforms to nano-sized Al_2O_3 particles which sinter at temperatures > 1200 °C.

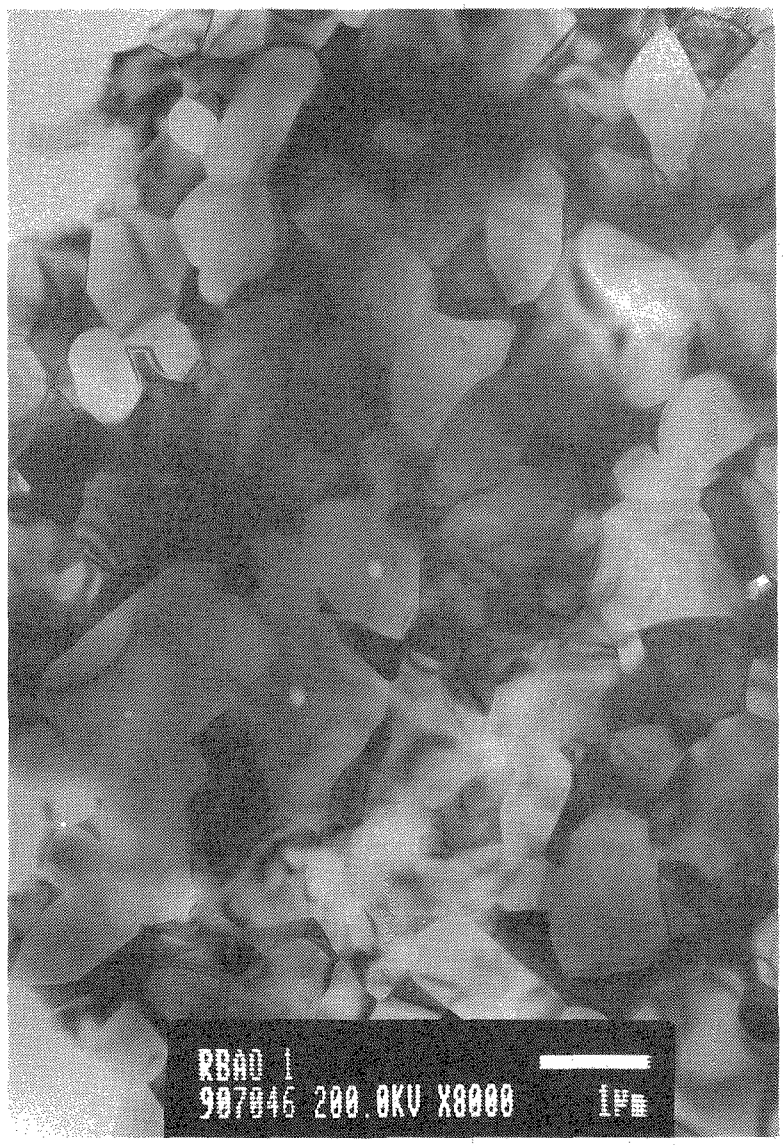

Fig. 2. TEM photograph of a thinned green body showing "old" and "new" Al_2O_3 particles contained in heavily deformed Al.

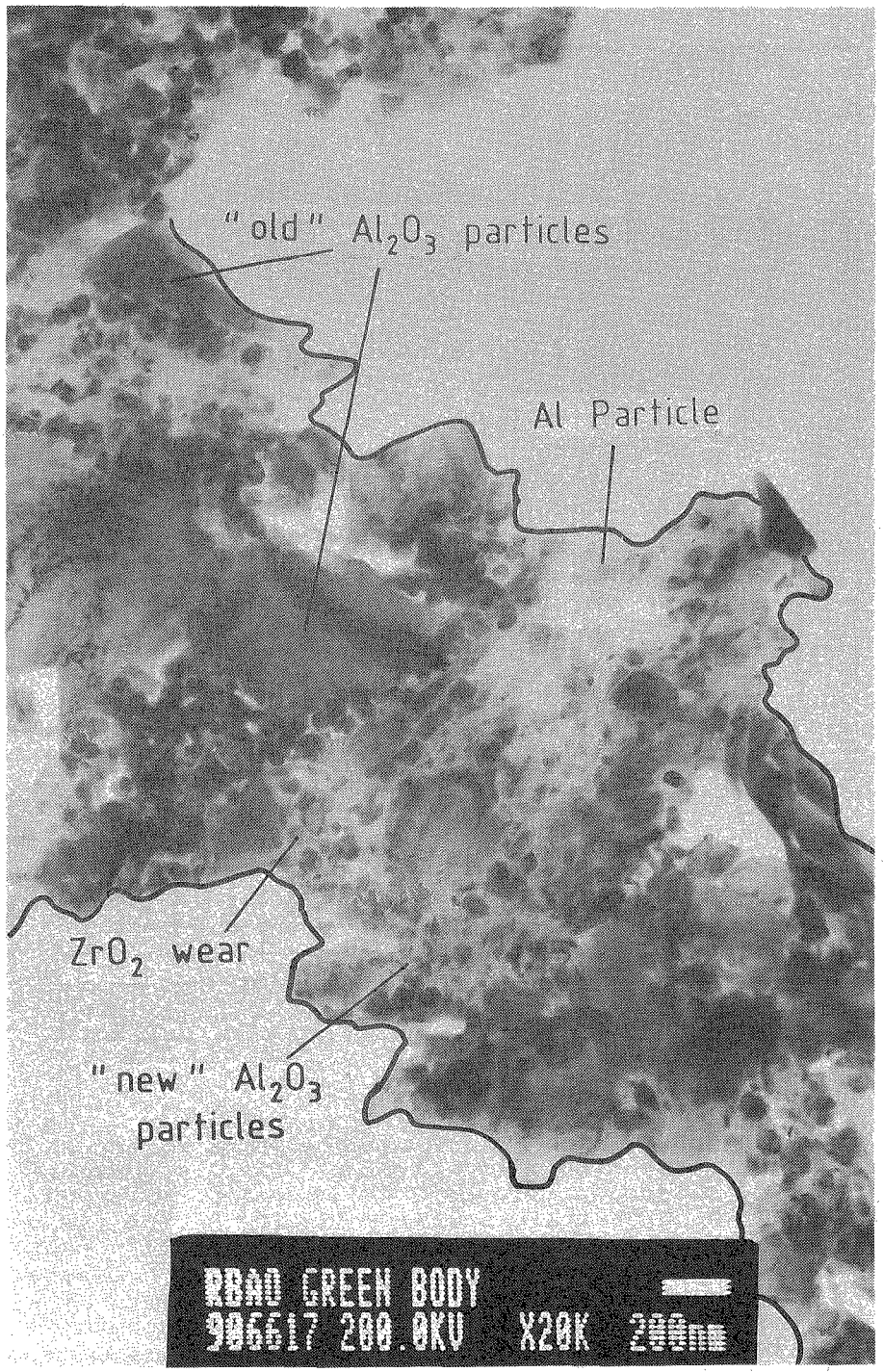

Fig. 3. Microstructure of ZrO_2-toughened RBAO reaction sintered at 1600°C for 5 h.

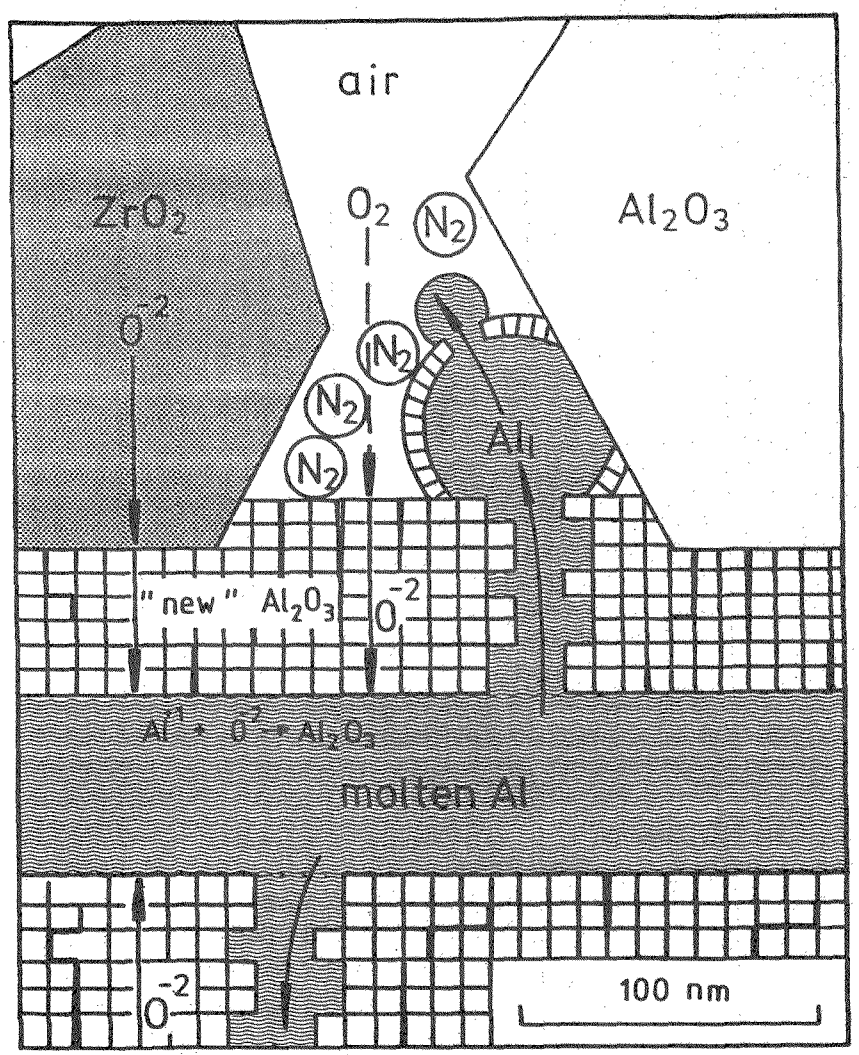

Fig. 4. Suggested mechanism for reaction of molten Al. Oxygen is transported either through the gas phase or by lattice diffusion through ZrO_2 particles to the Al particle. The high grain boundary density of the newly formed Al_2O_3 crystals represent the further fast pathway to the Al melt. Due to the increasing pressure in the confined Al particle, resulting from the 28 % volume expansion on reaction, the Al_2O_3 scale ruptures and liquid Al spills into the void space.

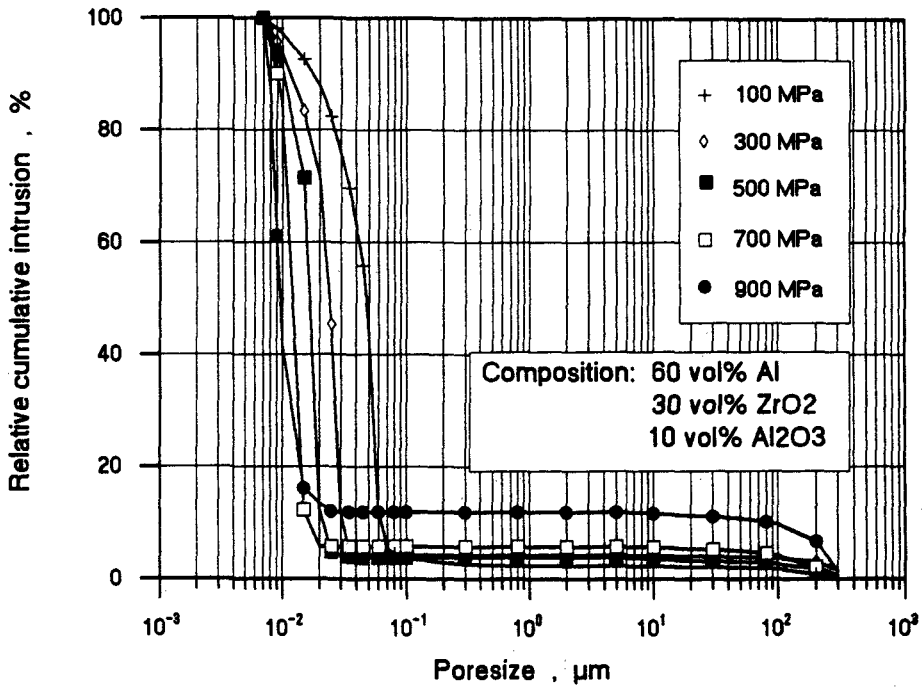

Fig. 5. Pore size distribution of RBAO green bodies as function of compaction pressure.

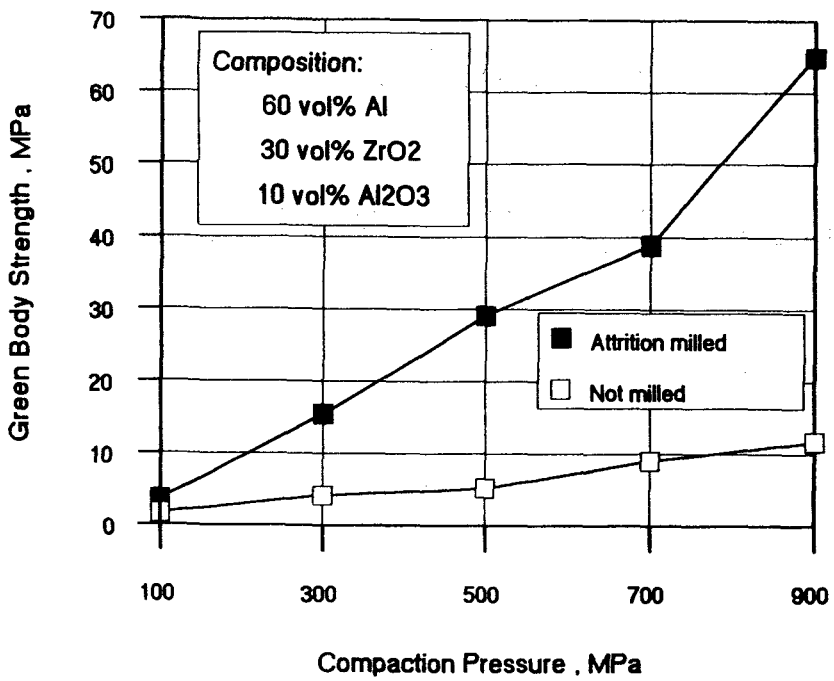

Fig. 6. Green body strength versus compaction pressure.

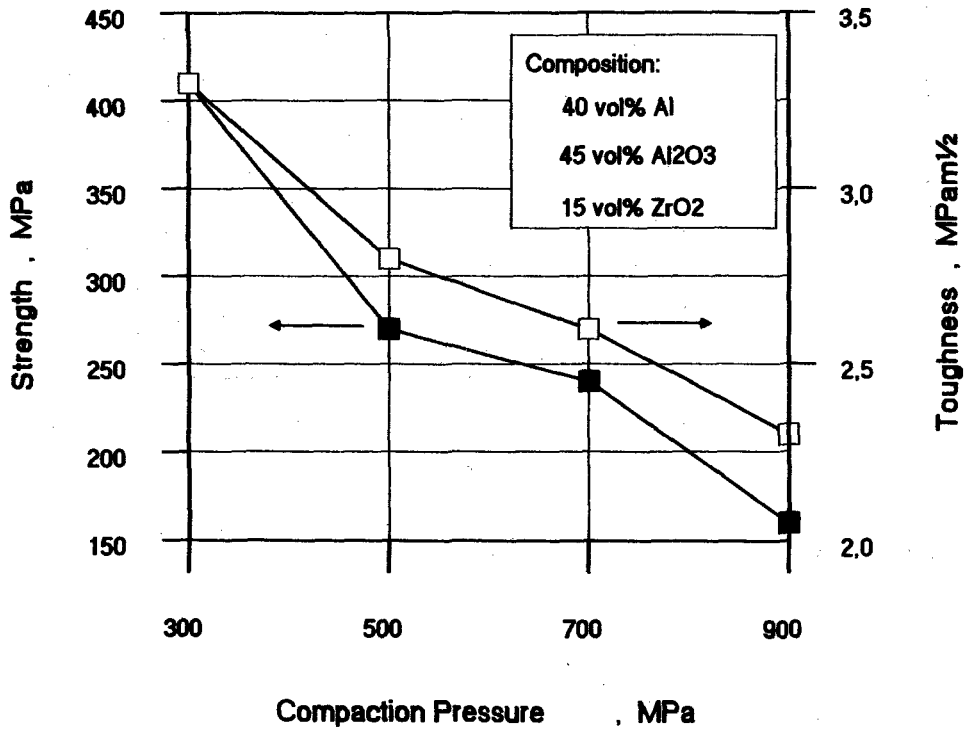

Fig. 7. Strength and toughness of RBAO with unstabilized ZrO_2 versus compaction pressure.